

# The possible counteractive effect of gold nanoparticles against streptozotocin-induced type 1 diabetes in young male albino rats

Manar E Selim<sup>1\*</sup>, Awatif A Hendi<sup>2</sup> and Ebtesam Alfalaj<sup>2</sup>

<sup>1</sup>Zoology Department, Faculty of Science, King Saud University, Ain Shams University, Cairo, Egypt

<sup>2</sup>Physics Department, Faculty of Science, King Saud University, Riyadh, Kingdom of Saudi Arabia

**Abstract:** The current study was performed to study the effect of biologically synthesised gold nanoparticles (AuNPs) to control hyperglycaemic conditions in streptozotocin (STZ)-induced diabetic mice. In this study, the rats were divided into four groups: Group I normal control rats (non-diabetic, untreated); Group II diabetes-induced rats used as diabetic controls DC (diabetic, untreated). Group III diabetes-induced rats treated with AuNPs DT; Group IV normal rats treated with AuNPs NT. Diabetes was induced by administering an intraperitoneal injection of a freshly prepared solution of STZ (50mg/kg body weight (bw)). The glucose level was significantly increased in the diabetic control rats compared with the controls ( $P < 0.001$ ). Decreased liver function and kidney function were detected in the diabetic treated rats and normal treated rats after AuNP administration compared with the controls. The present study is the first to demonstrate that AuNPs significantly enhance antioxidant production in STZ-induced diabetic rats, a recognised model of type 1 diabetes mellitus (T1DM).

**Keywords:** Gold nanoparticles; T1DM; antioxidant; rats.

## INTRODUCTION

Diabetes mellitus is a metabolic disease characterised by hyperglycaemia with impaired metabolism of glucose and other energy-yielding fuels, such as lipids and proteins (Scheen, 1997). This metabolic disorder is caused by a deficiency in insulin secretion or a resistance to insulin action, or both (Vinik A, Vinik E, 2003). Approximately 230 million people worldwide have been affected by diabetes, and approximately 366 million people are expected to be affected by 2030 (Wild *et al.*, 2004). Diabetic patients also exhibit oxidative stress, which leads to lipid per oxidation and tissue damage, including retinopathy, nephropathy and coronary heart disease (Wolffe *et al.*, 1991). Dyslipidaemia or hyperlipidaemia is also involved in the development of cardiovascular complications, which are a major cause of morbidity and mortality (Reasner, 2008).

Aronson 2008 reported that several pathogenic pathways are activated in diabetes, among which reactive oxygen species (ROS) generated by high glucose levels are responsible for many metabolic abnormalities and chronic complications. Other authors have reported that a counteractive defence system that eliminates the ROS produced during normal oxidative metabolism is maintained and that any imbalance in the production and scavenging of ROS leads to excessive levels of either molecular oxygen or ROS, thereby causing increased 'oxidative stress' (Harrison, 2003). Numerous studies have demonstrated that oxidative stress, mediated mainly by the hyperglycaemia-induced generation of free radicals, contributes to the development and progression

of diabetes and its complications; thus, antioxidant use may be an effective strategy to treat oxidative stress. The incidence of diabetes has soared worldwide in recent years and is expected to continue to rise, with the greatest increase observed in metabolic forms of diabetes. This finding is blamed largely on the rise in obesity and the global spread of Western-style habits, specifically, physical inactivity along with a diet that is high in calories, processed carbohydrates and saturated fats as well as insufficient in fibre-rich whole foods. Aging of the population is also a factor. However, other factors, such as the environment, may also contribute because cases of autoimmune diabetes (type 1) are also becoming more common. The estimated number of people with diabetes has increased markedly from 30 million in 1985 to 150 million in 2000 and then to 246 million in 2007, according to the International Diabetes Federation, which expects this number to reach 380 million by 2025. Seven percent of Americans have diabetes, according to the Centers for Disease Control and Prevention (CDC), which predicts that one in three Americans born in 2000 will eventually become diabetic. Health agencies are warning that diabetes is becoming an unprecedented epidemic, even as other major diseases (including cancer and non-diabetic heart disease) are being controlled. Gold compounds have received substantial attention as anti-inflammatory agents because of their ability to inhibit the expression of nuclear factor-kappaB (NF- $\kappa$ B) and decrease subsequent inflammatory reactions (Norton, 2008, Jeon *et al.*, 2003 and Lee *et al.*, 2007). The major drawback of ionic gold lies in the fact that it is easily inactivated by complexation and precipitation, thereby limiting its desired functions in the human system. Gold nanoparticles may be a valuable alternative to replace the

\*Corresponding author: e-mail: manar.selim@hotmail.com

potential of metallic gold (Kalishwaralal *et al.*, 2009). Guo *et al.* 2005 reported that gold nanoparticles (AuNPs), an emerging nanomedicine, are renowned for their promising therapeutic possibilities due to their significant properties such as biocompatibility, high surface reactivity, resistance to oxidation and surface plasmon resonance capability. The inhibitory activity of AuNPs toward the vascular permeability factor/vascular endothelial growth factor (VPF/VEGF165)-induced proliferation of endothelial cells provides clear evidence of their therapeutic potential in the treatment of diseases such as chronic inflammation, pathological neo-vascularisation, rheumatoid arthritis and neoplastic disorders (Mukherjee *et al.*, 2005). Hence, the effects of biologically synthesised AuNPs on streptozotocin (STZ)-induced diabetic (type 1) rats under hyperglycaemic conditions leading to oxidative stress were examined in this study.

## METHODS

### *Optical and electronic properties of AuNPs*

The interaction of AuNPs with light is strongly dictated by their environment, size and physical dimensions. The oscillating electric fields of a light ray propagating near a colloidal nanoparticle interact with the free electrons, causing a concerted oscillation of the electron charge that is in resonance with the frequency of the visible light. These resonant oscillations are known as surface plasmons. For small (~30nm) monodispersed AuNPs, the surface plasmon resonance phenomenon causes the absorption of light in the blue-green portion of the spectrum (~450nm), while red light (~700nm) is reflected, yielding a rich red colour. As the particle size increases, the wavelength of the surface plasmon resonance-related absorption shifts to longer, redder wavelengths. Red light is then absorbed and blue light is reflected, yielding solutions with a pale blue or purple colour (fig. 10). As the particle size continues to increase toward the bulk limit, the surface plasmon resonance wavelengths move into the infrared (IR) portion of the spectrum, and most visible wavelengths are reflected, giving the nanoparticles a clear or translucent colour. The surface plasmon resonance can be tuned by varying the size or shape of the nanoparticles, leading to particles with tailored optical properties for different applications.

This phenomenon is also observed when excess salt is added to the gold solution. The surface charge of the AuNPs becomes neutral, causing the nanoparticles to aggregate. Consequently, the solution's colour changes from red to blue. To minimise aggregation, the versatile surface chemistry of AuNPs allows them to be coated with polymers, small molecules and biological recognition molecules. This surface modification enables AuNPs to be used extensively in chemical, biological, engineering and medical applications. Typical properties of AuNPs are presented in table 4.

### *Surface plasmon absorption property of AuNPs*

AuNPs show a strong absorption band in the visible region when the frequency of the electromagnetic field is resonant with the coherent electron motion, which is called surface plasmon resonance absorption. The surface plasmon absorption results from the dipole oscillations of the free electrons with respect to the ionic core of a spherical nanoparticle. A net charge difference is shown on the nanoparticle surface when there is an interaction with an electric field, which causes polarisation of the electrons with respect to the ionic core of the nanoparticle (fig. 11).

### *Surface plasmon light-scattering property of AuNPs*

It is known that gold particle suspensions scatter coloured light when illuminated by a beam of white light. Light-scattering AuNP suspensions have the same appearance as fluorescent solutions, as shown in fig. 12. The light scattering is sensitive to the size, shape and composite of the nanoparticles and the comparison of the calculated intensity of the light scattered at 90° by AuNPs is shown in table 5. AuNPs of 58nm in diameter scatter green light, while those 78nm in diameter scatter yellow light (fig. 12). The scattered light from AuNPs is shown in fig. 13 (Kneipp *et al.*, 2005).

### *Characterisation of the AuNPs*

The morphology and size of the biologically synthesised AuNPs was determined using transmission electron microscopy (TEM), as shown in fig. 14. The images clearly show that the average size of the particles was on the order of 20 nm and that they were relatively uniform in diameter and spherical in shape. The Lal test revealed that the synthesised nanoparticles were endotoxin free based on the qualitative analysis, which did not demonstrate any formation of gel clots. Atomic force microscopy (AFM) or scanning force microscopy (SFM) is a very high-resolution type of scanning probe microscopy, with a demonstrated resolution of approximately fractions of a nanometre, which is more than 1000 times better than the optical diffraction limit, as shown in fig. 15. The size of the synthesised spherical AuNPs was analysed through a zeta sizer. The concentration of the spherical AuNPs was  $5.078 \times 10^{-4}$  molar. Furthermore, the number of spherical AuNP atoms was  $30.57 \times 10^{19}$  atoms.

### *Quality advantage*

Aldrich Materials Science, in conjunction with Cytodiagnosics, is proud to offer a broad portfolio of AuNPs geared specifically for high-technology applications within the fields of life science and materials science. AuNPs are available in sizes ranging from 5 nm to 400nm in diameter, with numerous surface functionalities in a variety of solvent compositions. While spherical AuNPs are traditionally synthesised using reducing agents such as sodium citrate or sodium borohydride, Cytodiagnosics has a propriety process and

formulation that leads to the preparation of highly spherical AuNPs without harsh reducing agents. Compared with other AuNPs, these nanoparticles have many advantages, including the following:

1. Narrow size distribution based on Dynamic Light Scattering (DLS) and TEM analysis.
2. Consistent size and shape - <10% CV (coefficient of variance) even above 100 nm. Examples of 5 nm and 400 nm nanoparticles are shown below in fig. 16.

### Selection of animals

The study was conducted on male albino rats, 8 to 9 weeks of age, weighing 95±5g, housed in polycarbonate cages (five rats per cage) at an ambient temperature of 25 ±2°C with 12 h-light and 12 h-dark cycles. The rats were fed with commercially obtained rodent chow and water *ad libitum*. The animals were allowed to acclimatise to the laboratory environment and then they were randomly subjected to the experiment. All of the animal experiments were conducted in the Medical College animal house at King Khalid University Hospital (King Saud University).

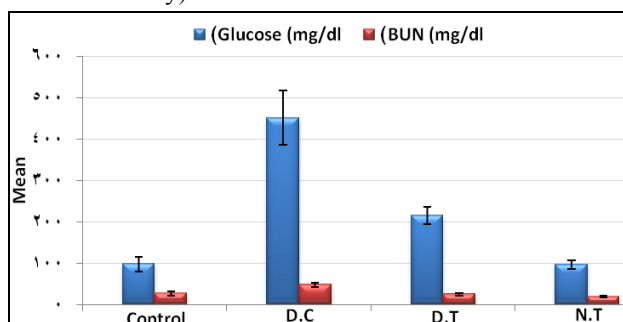


**Fig. 1:** Means (with SD error bars) of the glucose (mg/dL) and BUN (mg/dL) levels in the different groups.

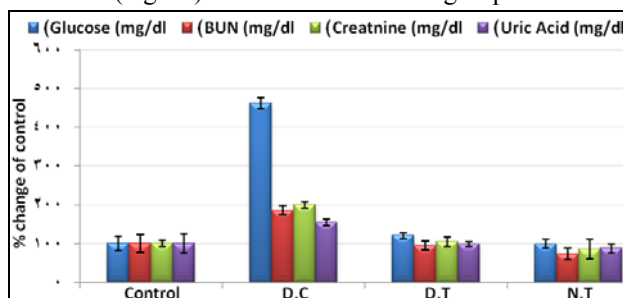


**Fig. 2:** Means (with SD error bars) of the glucose (mg/dL) and BUN (mg/dL) levels in the different groups.

### Dosage optimisation

Based on the assessment made on the final day, the effective inhibitor dosage (EC<sub>50</sub>) of 2.5mg/kg bw/day of AuNPs, which reduced the blood glucose level significantly [data not shown] in comparison with other dosages, was fixed as the optimum dosage and the subsequent studies were conducted at this dose.

### Experimental design

The rats were divided into four groups (n=10 rats per group) as follows:

- Group I Normal control rats (non-diabetic, untreated).
- Group II Diabetes-induced rats used as the diabetic control - DC (diabetic, untreated).
- Group III Diabetes-induced rats treated with AuNPs - DT (diabetic, treated)
- Group IV Normal rats treated with AuNPs - NT (non-diabetic, treated)

### Induction of diabetes mellitus and treatment with AuNPs

Diabetes was induced by administering an intraperitoneal injection of a freshly prepared solution of STZ (50 mg/kg bw) in 0.1 M cold citrate buffer (pH 4.5) to the overnight-fasted rats of Group II and Group III. Because of the instability of STZ in aqueous media, the solution was made using cold citrate buffer (pH 4.5) immediately prior to administration. The rats were allowed to drink a 5% glucose solution overnight to overcome the drug-induced hypoglycaemia. The blood glucose values were measured to be above 250mg/dL on the third day after STZ injection, thus confirming the induction of diabetes in the rats. Once the hyperglycaemic condition was confirmed, the treatment was begun on the 5<sup>th</sup> day after STZ injection, and it was considered as the 1<sup>st</sup> day of treatment. The AuNPs were administered to each rat in Group III and Group IV at a dosage of 2.5mg/kg bw/day through intraperitoneal injection using a tuberculin syringe for 45 days, while the control group received citrate buffer alone.

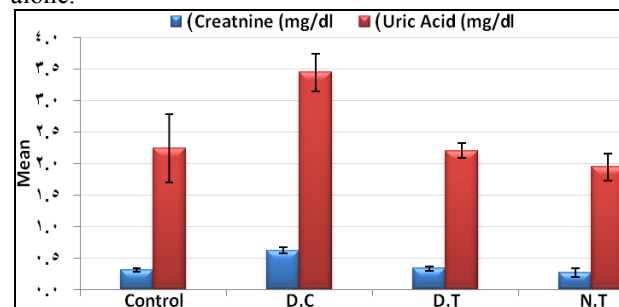


**Fig. 3:** Means (with SD error bars) of the creatinine (mg/dL) and uric acid (mg/dL) in the different groups.

### Oral glucose tolerance test (OGTT)

The OGTT was performed after the treatment with AuNPs in Groups III and IV for 45 days to study the control effect of AuNPs in glucose-induced tolerance. The rats were fasted overnight and blood was collected from the tip of the tail vein to determine the FBG level. The OGTT was performed by orally administering glucose at approximately 1g/kg bw dissolved in 0.1mL of clean water to the overnight-fasted animals. At various time intervals of 30, 60, 90 and 120 min after the oral glucose load, blood samples were collected from the tail vein with potassium oxalate and sodium fluoride to estimation the glucose levels. The blood glucose values were expressed in mg/dL of blood.

### **Euthanasiation of experimental animals**

After completion of the FBG and OGTT, the rats from all of the experimental groups were deprived of food overnight and euthanised by cervical dislocation under ketamine-xylazine anaesthesia. Blood and organ samples were collected carefully for various biochemical measurements.

### **Estimation of blood glucose and urea**

The blood samples collected by cardiac puncture using sterile vials were immediately used to estimate the blood glucose level using the glucose oxidase-peroxidase (GOD-POD) glucose estimation kit. The values are expressed as mg/dL. The level of urea in the plasma was estimated by the method described earlier (Calam, 1988). Briefly, 3.3 mL of water, 0.3 mL of 10% sodium tungstate and 0.3 mL of 0.67 N sulphuric acid were added to 0.1 mL of plasma. The suspensions were centrifuged and 0.4 mL of diacetylmonoxime and 2.6 mL of sulphuric acid-phosphoric acid were added in that order to 1 mL of supernatant. Standard urea (20-50 µg/mL) was also treated in a similar manner and heated in a boiling water bath for 30 min, then cooled, and the developed colour was measured at 480 nm. The values are expressed as mg/dL of plasma.

### **Serum analysis**

Whole blood was placed in a clotted vial and centrifuged. The collected serum was submitted to an automated analyser (Micro Lab 300: Merck, Netherlands) for biochemical analysis. The serum biochemical analysis was conducted to determine the levels of metabolic enzymes such as AST, ALT and ALP to assess liver function and the creatinine, BUN and uric acid levels to assess renal function.

### **Measurement of antioxidant enzymes: SOD, CAT, GSH and GPx activities**

The antioxidant system comprises several enzymes such as CAT, SOD, GSH, and GPx that are responsible for maintaining a balanced system of oxidation reactions and thereby inhibiting an increase in oxidative stress (Tietz, 1987). The SOD activity was measured according to a previously described method (Nishikimi *et al.*, 1972). Briefly, the reaction mixture (2.1 mL) contained 1924 µL sodium carbonate buffer (50 mM), 30 µL nitroblue tetrazolium (1.6 mM), 6 µL Triton X-100 (10%) and 20 µL hydroxylamine-HCl (100 mM). Subsequently, 100 µL of enzyme was added, and the absorbance (560 nm) was read for 5 min against the blank (reaction mixture without an enzyme source). The change in the absorbance was calculated per minute (i.e.,  $\Delta 560$ ) and used to estimate the enzyme activity. This assay relies on the ability of the enzyme to inhibit the phenazine methosulphate-mediated reduction of nitroblue tetrazolium dye. The GR content was measured as described previously (Goldberg and Spooner, 1983). Briefly, the reaction mixture containing 1.2 mL ethylenediaminetetraacetic acid (EDTA) (0.02 M),

1 mL distilled water, 250 µL 50% trichloroacetic acid (TCA) and 50 µL Tris buffer (0.4 M, pH 8.9) was centrifuged at 300 x g for 15 min. The clear supernatant (500 µL) was mixed with 1 mL of 0.4 M Tris buffer (containing 0.02 M EDTA, pH 8.9), 100 µL of 0.01 M DTNB (5, 5'-dithio-bis-(2-nitrobenzoic acid)) and 100 µL enzyme source. The mixture was incubated at 37°C for 25 min. The yellow colour that developed was read at 412 nm against a blank. GR catalyses the reduction of glutathione (GSSG) in the presence of NADPH, which is oxidised to NADPH<sup>+</sup>. The decrease in absorbance at 340 nm was measured. GR: NADPH + H<sup>+</sup> + GSSG = NADP<sup>+</sup> + 2GSH. The level of CAT was assayed according to the method described previously (Aebi, 1984 and Fossati *et al.*, 1980). Briefly, 1.2 mL of phosphate buffer was added to 0.2 mL of the serum, and the enzyme reaction was initiated by the addition of 1.0 mL of H<sub>2</sub>O<sub>2</sub> solution. The decrease in the absorbance was measured at 420 nm at 30-second intervals for one minute. The enzyme blank was run simultaneously with 10 mL of distilled water instead of hydrogen peroxide. The enzyme activity was expressed as µmoles of H<sub>2</sub>O<sub>2</sub> decomposed/min/mg protein. CAT reacts with a known quantity of H<sub>2</sub>O<sub>2</sub>. The reaction is stopped after exactly one min, using a catalase inhibitor. CAT: 2H<sub>2</sub>O<sub>2</sub> = 2 H<sub>2</sub>O + O<sub>2</sub>. In the presence of peroxidase (HRP), the remaining H<sub>2</sub>O<sub>2</sub> reacts with 3, 5-dichloro-2-hydroxybenzene sulfonic acid (DHBS) and 4-aminophenazone (AAP) to form a chromophore with a colour intensity inversely proportional to the amount of CAT in the original sample. HRP: 2H<sub>2</sub>O<sub>2</sub> + DHBS + AAP = Quinoneimine Dye + 4 H<sub>2</sub>O. The GPx activity was assayed according to the method described previously (Paglia, 1967). Briefly, the reaction mixture consisted of 0.2 mL of EDTA, 0.1 mL of sodium azide, 0.1 mL of H<sub>2</sub>O<sub>2</sub>, 0.2 mL of GSH, 0.4 mL of phosphate buffer and 0.2 mL tissue homogenate, which were incubated at 37°C for 10 min. The reaction was arrested by the addition of 0.5 mL of TCA and the tubes were centrifuged at 5000 rpm; the colour that developed was read at 420 nm immediately. The enzyme activity was expressed as µmoles of GSH oxidised/min/mg protein. The assay is an indirect measure of the activity of c-GPx. GSSG, produced upon reduction of an organic peroxide by c-GPx, is recycled to its reduced state by the enzyme GR. c-GPx: ROOH + 2GSH = ROH + GSSG + H<sub>2</sub>O. GR: GSSG + NADPH + H<sup>+</sup> = 2GSH + NADP<sup>+</sup>. The oxidation of NADPH to NADP<sup>+</sup> is accompanied by a decrease in the absorbance at 340 nm (A<sub>340</sub>), providing a spectrophotometric means for monitoring the GPx enzyme activity. The molar extinction coefficient for NADPH is 6220 M<sup>-1</sup> cm<sup>-1</sup> at 340 nm. To assay c-GPx, a cell or tissue homogenate is added to a solution containing GSH, GR and NADPH. The enzyme reaction is initiated by adding the substrate (H<sub>2</sub>O<sub>2</sub>), and the A<sub>340</sub> is recorded. The rate of the decrease in the A<sub>340</sub> is directly proportional to the GPx activity in the sample.

**Table 1:** Comparison between the control, DC, DT and NT groups with respect to the ALT (U/L), AST (U/L) and ALP (U/L) levels.

Parameters	Groups	N	Mean $\pm$ SD	P value <sup>a</sup>	P value <sup>b</sup>	P value <sup>c</sup>	Percent change compared with control
ALT (U/L)	Control	5	54.20 $\pm$ 12.11	-----	-----	<0.001	100.00
	DC	5	168.80 $\pm$ 11.14	<0.001	<0.001		311.44
	DT	5	67.40 $\pm$ 5.98	>0.05	>0.05		124.35
	NT	5	79.20 $\pm$ 17.28	<0.05	-----		146.13
AST (U/L)	Control	5	137.20 $\pm$ 38.04	-----	-----	<0.05	100.00
	DC	5	510.80 $\pm$ 269.51	<0.05	<0.05		372.30
	DT	5	172.00 $\pm$ 25.90	>0.05	>0.05		125.36
	NT	5	99.60 $\pm$ 13.13	>0.05	-----		72.59
ALP (U/L)	Control	5	265.00 $\pm$ 50.76	-----	-----	<0.001	100.00
	DC	5	897.00 $\pm$ 96.81	<0.001	<0.001		338.49
	DT	5	397.20 $\pm$ 20.74	<0.001	<0.001		149.88
	NT	5	223.80 $\pm$ 32.24	>0.05	-----		84.45

Table 1 describes the following: The independent t-test between the control group and the DC, DT and NT groups with respect to the ALT (U/L), AST (U/L) and ALP (U/L) levels.

The independent t-test between the DC group and the DT group with respect to the ALT (U/L), AST (U/L) and ALP (U/L) levels

The one-way ANOVA between the control, DC, DT and NT groups with respect to the ALT (U/L), AST (U/L) and ALP (U/L) levels.

Percent change compared with the control with respect to the ALT (U/L), AST (U/L) and ALP (U/L) levels.

**Table 2:** Comparison between the control, DC, DT and NT groups with respect to the SOD (U/mL), CAT (U/mL), GPx (U/L) and GR (U/L) levels.

Parameters	Groups	N	Mean $\pm$ SD	P value <sup>a</sup>	P value <sup>b</sup>	P value <sup>c</sup>	Percent change compared with control
Superoxide Dismutase (U/mL)	Control	5	13.18 $\pm$ 1.39	-----	-----	<0.001	100.00
	DC	5	3.17 $\pm$ 0.12	<0.001	<0.001		24.05
	DT	5	19.54 $\pm$ 2.62	<0.001	<0.001		148.23
	NT	5	43.16 $\pm$ 10.09	<0.001	-----		327.42
Catalase (U/mL)	Control	5	0.21 $\pm$ 0.01	-----	-----	<0.001	100.00
	DC	5	0.14 $\pm$ 0.004	<0.001	<0.001		64.68
	DT	5	0.43 $\pm$ 0.02	<0.001	<0.001		199.25
	NT	5	0.50 $\pm$ 0.07	<0.001	-----		235.23
Glutathione Peroxidase (U/L)	Control	5	39.82 $\pm$ 2.07	-----	-----	<0.001	100.00
	DC	5	19.16 $\pm$ 1.44	<0.001**0.001	<0.001		48.12
	DT	5	70.58 $\pm$ 7.58	<0.001	<0.001		177.27
	NT	5	83.77 $\pm$ 6.59	<0.001	-----		210.38
Glutathione Reductase (U/L)	Control	5	2.00 $\pm$ 0.12	-----	-----	<0.001	100.00
	DC	5	0.70 $\pm$ 0.06	<0.001	<0.001		35.08
	DT	5	1.58 $\pm$ 0.14	<0.001	<0.001		78.64
	NT	5	1.87 $\pm$ 0.11	>0.05	-----		93.41

(Significance level: P<0.05\*, significant P<0.01\*\*, highly significant)

<sup>a</sup>P value between the control group and the DC, DT and NT groups, <sup>b</sup>P value between the DC group and the DT group, <sup>c</sup>P value between the control, DC, DT and NT groups

Table 2 describes: The independent t-test between the control group and the DC, DT and NT groups with respect to the SOD (U/mL), CAT (U/mL), GPx (U/L) and GR (U/L) levels.

The independent t-test between the DC group and the DT group with respect to the SOD (U/mL), CAT (U/mL), GPx (U/L) and GR (U/L) levels.

The one-way ANOVA between the control, DC, DT and NT groups with respect to the SOD (U/mL), CAT (U/mL), GPx (U/L) and GR (U/L) levels.

Percent change compared with the control with respect to the SOD (U/mL), CAT (U/mL), GPx (U/L) and GR (U/L) levels.

**Table 3:** Typical properties of AuNPs

Diameter	Nanoparticles/ml	Peak SPR Wavelength	Molar Ext $M^{-1} cm^{-1}$	
5nm	$5.47 \times 10^{13}$	515-520nm	$1.10 \times 10^7$	Surfactant Stabilized PBS
10nm	$5.98 \times 10^{12}$	515-520nm	$1.01 \times 10^8$	Surfactant Stabilized PBS
20nm	$6.54 \times 10^{11}$	524nm	$9.21 \times 10^8$	Surfactant Stabilized PBS
30nm	$1.79 \times 10^{11}$	526nm	$3.36 \times 10^9$	Surfactant Stabilized PBS
40nm	$7.15 \times 10^{10}$	530nm	$8.42 \times 10^9$	Surfactant Stabilized PBS
50nm	$3.51 \times 10^{10}$	535nm	$1.72 \times 10^{10}$	Surfactant Stabilized PBS
60nm	$1.96 \times 10^{10}$	540nm	$307 \times 10^{10}$	Surfactant Stabilized PBS
80nm	$7.82 \times 10^9$	553nm	$7.70 \times 10^{10}$	Surfactant Stabilized PBS
100nm	$3.84 \times 10^9$	572nm	$1.57 \times 10^{11}$	Surfactant Stabilized PBS
150nm	$3.60 \times 10^9$	Not Measured	-	

### STATISTICAL ANALYSIS

Values are expressed as the mean  $\pm$  standard deviation (SD). The statistical significance was evaluated by one-way analysis of variance (ANOVA) followed by Student's t test at a 5% level of significance compared with the control ( $P < 0.05$ ) (Graph Pad, San Diego, CA).

### RESULTS

#### Blood analysis

##### Mean glucose level (mg/dL)

As shown in table 1 and fig. 1, the mean glucose level was significantly increased in the DC rats compared with the control rats (450.80 vs. 97.60mg/dL;  $P < 0.001$ ). Moreover, there was a significant difference in the mean glucose level between Group II rats compared with Group III DT rats (450.80 vs. 214.60mg/dL;  $P < 0.001$ ). However, treatment with AuNPs in the Group IV NT rats did not significantly lower the mean glucose level, and there was no significant difference compared with the control rats (96.20 vs. 97.60 mg/dL;  $P > 0.05$ ). This result suggests that the AuNPs maintained the blood glucose level near the control level. In addition, the NT rats had a mean level of glucose that was 98.57% of the control level, which was very close (fig. 2).

##### Mean blood urea nitrogen (BUN) level (mg/dL)

As shown in table 1 and fig. 1, a decrease in the mean BUN level was detected in the DT rats and NT rats compared with the controls (25.20 and 18.80, respectively, vs. 26.60mg/dL). In addition, a significant increase in the BUN level was found in the DC rats

compared with the control rats (47.60 vs. 26.60mg/dL;  $P < 0.001$ ). However, no significant change was detected in the DC rats compared with the control rats (25.20 vs. 26.60mg/dL;  $P > 0.05$ ). The percentage change between the control (fig. 2) and Groups III and IV showed a decreased BUN level (94.73% and 73.44% of the control level, respectively), thereby confirming the protective role of AuNPs in STZ-induced diabetic rats.

**Table 4:** Comparison of the calculated intensity of light scattered at  $90^\circ$  by gold particles illuminated with monochromatic ( $I_u$ ) and white unpolarised light ( $I_u, INT$ ).

Diameter (nm)	$I_{U,INT}(90)$	$I_U(90)^a$
20	1	1
40	71.3	72.5
60	859	973
80	$4.42 \times 10^3$	$5 \times 10^3$
100	$1.33 \times 10^4$	$1.5 \times 10^4$
120	$2.74 \times 10^4$	$3.1 \times 10^4$
140	$4.34 \times 10^4$	$4.92 \times 10^4$
160	$5.79 \times 10^4$	$6.56 \times 10^4$

##### Creatinine level (mg/dL)

As shown in table 1 and fig. 3, STZ-induced diabetic rats (Group II) exhibited significantly increased creatinine levels compared with the control rats (0.62 vs. 0.31 mg/dL;  $P < 0.001$ ). Moreover, the DT rats and the NT rats did not show any significant changes compared with the control Group I rats (0.33 and 0.27, respectively, vs. 0.31 mg/dL;  $P > 0.05$ ).

A significant difference was observed between the DC rats and the DT rats (0.62 vs. 0.33mg/dL;  $P < 0.001$ ). The percentage change between the control and Group III rats demonstrated a partially increased level of creatinine (105.13%), but this marker was decreased in the Group IV rats (85.90%), which supports the protective role of AuNPs for kidney function (fig. 2).

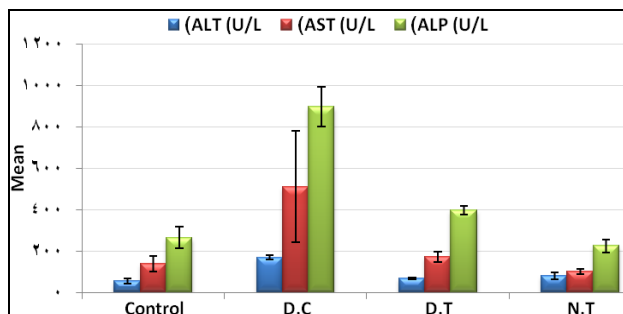


**Fig. 4:** Means (with SD error bars) of the ALT (U/L), AST (U/L) and ALP (U/L) levels in the different groups.

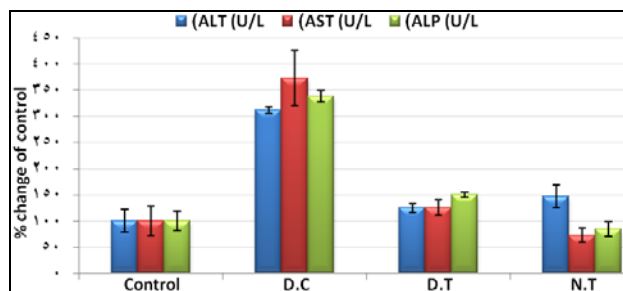


**Fig. 5:** Percentage change (with error bars) in the ALT (U/L), AST (U/L) and ALP (U/L) levels in the different groups.

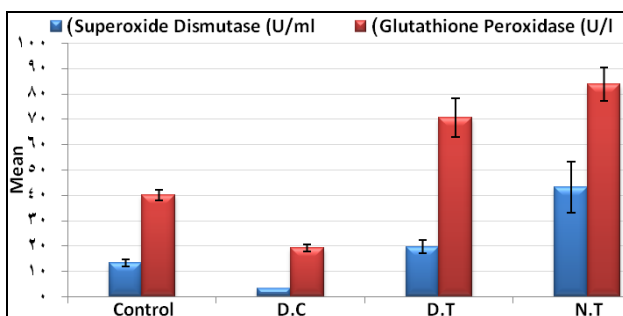


**Fig. 6:** Means (with SD error bars) of the SOD (U/mL) and GPx (U/L) levels in the different groups.

**Uric acid level (mg/dL)**

As shown in table 1 and fig. 3, treatment of the STZ-induced diabetic rats significantly increased the uric acid level compared with the control rats (2.20 vs. 2.24mg/dL;  $P < 0.001$ ). However, the DT rats in Group III and the NT rats in Group IV did not show any significant changes compared with the control Group I rats (2.20 and 1.94, respectively, vs. 2.24mg/dL;  $P > 0.05$ ). The uric acid level was significantly increased in the DC rats compared with the DT rats (3.44 vs. 2.20mg/dL;  $P < 0.05$ ). The DT and

NT rats exhibited decreased levels of uric acid (98.21% and 86.61% of the control level, respectively; fig. 2), but an increased level was recorded in the DC rats (153.57%). These results suggest the restorative effect of AuNPs on renal function.

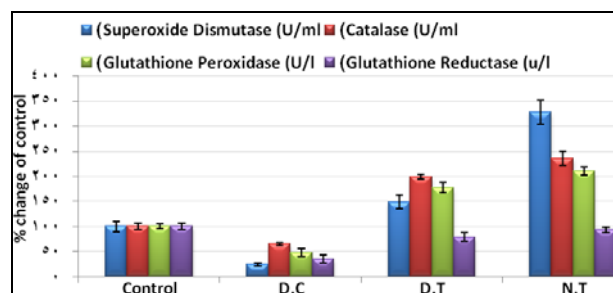


**Fig. 7:** Percentage change (with SD error bars) in the levels of SOD (U/mL), CAT (U/mL), GPx (U/L) and GR (U/L) in the different groups.

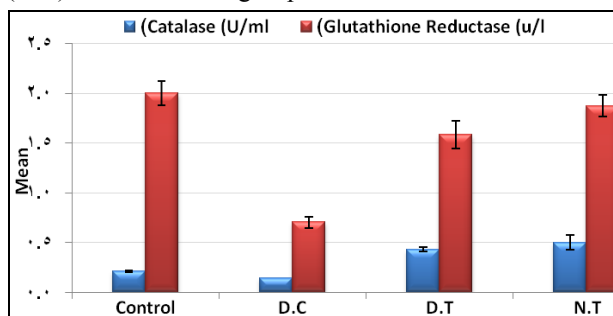
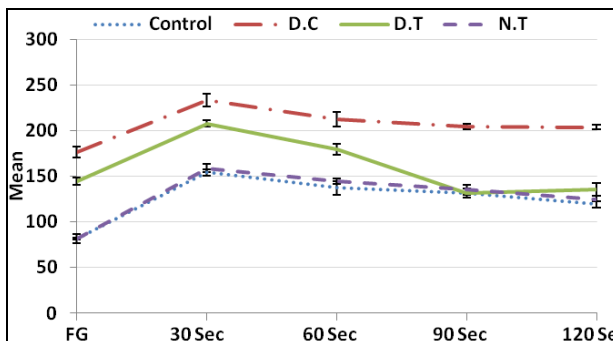


**Fig. 8:** Means (with SD error bars) of the CAT (U/mL) and GR (U/L) levels in the different groups.



The results are expressed as the means  $\pm$  SD of n = 10 rats. FBG, fasting blood glucose level in the different groups.

**Fig. 9:** The glucose tolerance results in STZ-induced diabetic rats in response to AuNP treatment.

**Serum analysis**

Enzymes such as aspartate aminotransferase (AST), alanine aminotransferase (ALT), and alkaline phosphates (ALP) are responsible for the proper functioning of the liver, and any damages induced in the liver due to hyperglycaemic conditions may lead to excessive leakage of these enzymes into the bloodstream. Thus, the effect of the AuNPs on the levels of the different metabolic enzymes measuring the effective functioning of the liver through the serum analysis were analysed, and the

protective effect of AuNPs against liver damage was demonstrated as follows:

1- As presented in table 2 and fig. 4, the enzyme ALT showed significantly elevated levels in the DC rats (Group II) compared with the control group (168.80 vs. 54.20 U/L;  $P < 0.001$ ). The ALT levels were partially increased in normal rats after treatment with AuNPs compared with the controls (79.20 vs. 54.20 U/L;  $P < 0.05$ ). When the effect of the AuNPs on the level of ALT (the effective functioning of the liver) was analysed through serum analysis, the protective effect of the AuNPs against liver damage as measured by the enzyme ALT level showed no significant elevation in the DT rats (Group III) compared with the control group (67.40 vs. 54.20 U/L;  $P > 0.05$ ). The percentage change between the control and Groups III and IV rats revealed partially increased ALT levels (124.35% and 146.13% of the control level, respectively), thus confirming the protective role of AuNPs in STZ-induced diabetic rats (fig. 5).



This phenomenon is also observed when excess salt is added to the gold solution. The surface charge of the gold nanoparticles becomes neutral, causing the nanoparticles to aggregate. Consequently, the solution's colour changes from red to blue. To minimise aggregation, the versatile surface chemistry of the AuNPs allows them to be coated with polymers, small molecules and biological recognition molecules. This surface modification enables the AuNPs to be used extensively in chemical, biological, engineering and medical applications. Typical properties of AuNPs are presented in table 4.

**Fig. 10:** Colours of various sized monodispersed AuNPs.

2- As shown in table 2 and fig. 4, hyperglycaemic conditions can cause excessive leakage of AST into the bloodstream. AST is responsible for the proper functioning of the liver and any damage induced in the liver due to hyperglycaemic conditions may lead to excessive leakage of this enzyme into the bloodstream. In the STZ-induced diabetic rats (Group II), the AST levels were significantly increased compared with the control group (510.80 vs. 137.20 U/L;  $P < 0.05$ ). Thus, treatment with AuNPs in non-diabetic or in diabetic rats lowered the levels of AST near to control levels. No significant change was observed in the Groups III and IV rats compared with the control group (99.60 and 172.00,

respectively, vs. 137.20 U/L;  $P > 0.05$ ). Moreover, a significant decrease in the AST level was detected in the DT rats compared with the DC rats (172.00 vs. 510.80 U/L;  $P < 0.05$ ). Following the treatment with AuNPs at a dosage of 2.5 mg/kg body weight (bw), the DT Group III rats presented a partial increase in AST levels as a percentage of the control compared with the DC Group II rats (125.36% vs. 372.30% as a percentage of the control level, respectively), which directly reveals the protective/regenerative effects of AuNPs with respect to the activity of the liver. Moreover, the NT rats exhibited a decreased change in this marker (72.59% as a percentage of the control level) (fig. 5).

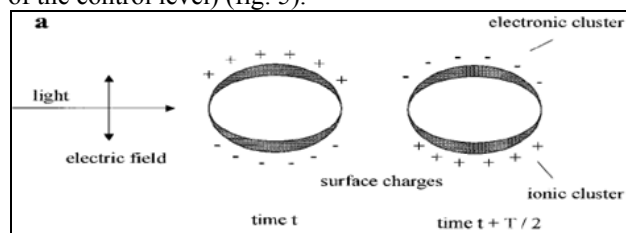


**Fig. 11:** A scheme of surface plasmon absorption of spherical nanoparticles illustrating the excitation of the dipole surface plasmon oscillation.

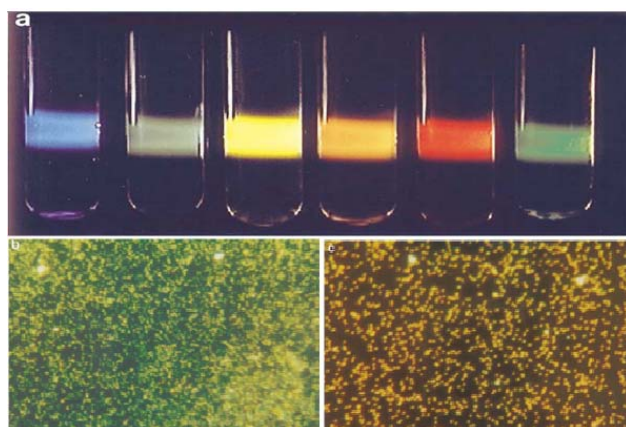


**Fig. 12:** a: The AuNPs of different sizes irradiated by a beam of white light; b: The light-scattering imaging of 58 nm AuNPs; c: The light-scattering imaging of 78 nm AuNPs.

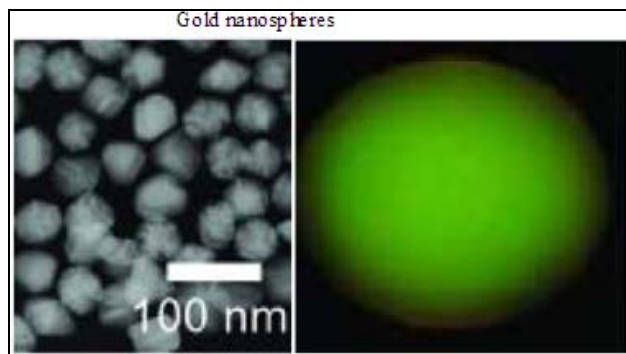


**Fig. 13:** Light scattering of gold nanospheres.

3- As shown in table 2 and fig. 4, the enzyme ALP showed significantly elevated levels in the DC Group II rats compared with the control group (897.00 vs. 265.00 U/L;  $P < 0.001$ ). The ALP levels were partially increased in the DT rats compared with the control rats (223.80 vs. 265.00 U/L;  $P < 0.05$ ). In contrast, the treatment with AuNPs lowered the level of ALP to near normal in the NT rats, and no significant difference was observed between the Group IV and the control group rats (223.80 vs. 265.00 U/L;  $P > 0.05$ ). These results indicate that the AuNP treatment was effective in lowering the mean ALP levels, as demonstrated in the Group III and Group IV ALP levels compared with the mean ALP levels in the DC rats. Additionally, a significant decrease in the ALP level was detected in the DT rats compared with the DC rats (397.20 vs. 897.00 U/L;  $P < 0.001$ ). The percentage change between the control and Group III rats revealed a partially increased ALP level (187.62% of the control level), but this marker was decreased in the Group IV rats (84.45% of the control level), supporting the protective effect of AuNPs on liver function (fig. 5).

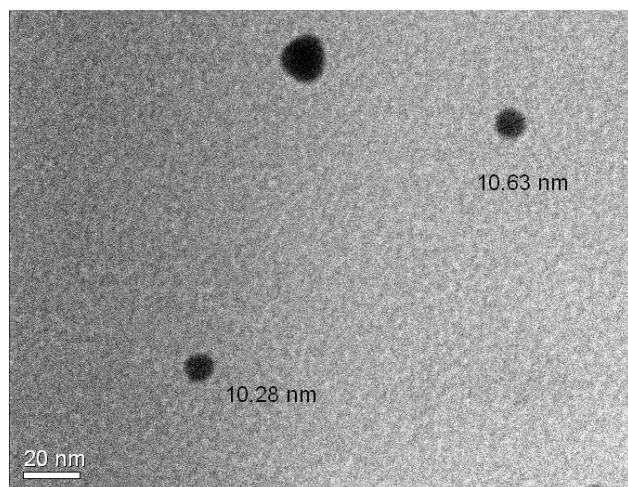


**Fig. 14:** TEM of spherical AuNPs.

#### **Antioxidant enzymes**

Glutathione (GSH) is a tripeptide with a free reductive thiol functional group that is responsible for the detoxification of peroxides such as hydrogen peroxide or lipid peroxides, and it acts as an important antioxidant in cells. During the detoxification process, GSH (in its reduced form) becomes oxidised glutathione (GSSG), which is then recycled to GSH by the enzyme glutathione reductase (GR) present in cells. The increased ROS levels in diabetes could be due to increased ROS production and/or decreased ROS destruction by antioxidants such as GSH, super oxide dismutase (SOD), catalase (CAT) and glutathione per oxidase (GPx).

#### **Super oxide dismutase (SOD) (U/mL)**

SODs are metalloenzymes that catalyse the dismutation of the super oxide anion to molecular oxygen and hydrogen

peroxide and thus form a crucial part of the cellular antioxidant defence mechanism.

1- As shown in table 3 and fig. 6, there was a significant decrease in SOD activity in the DC rats compared with the control rats (3.17 vs. 13.18 U/mL;  $P < 0.001$ ). However, administration of AuNPs to diabetic rats or to normal rats caused a significant increase in this marker compared with the control (43.16 and 19.54, respectively vs. 13.18 U/mL;  $P < 0.001$ ). After the use of AuNPs in the STZ-induced diabetic rats, a significant increase in the plasma SOD activity compared with the DC rats was observed (43.16 vs. 3.17 U/mL;  $P < 0.001$ ). Furthermore, the AuNP treatment was associated with increased SOD activity (fig. 7) in the Groups III and IV rats (148.23% and 327.42% as a percentage of the control level, respectively).

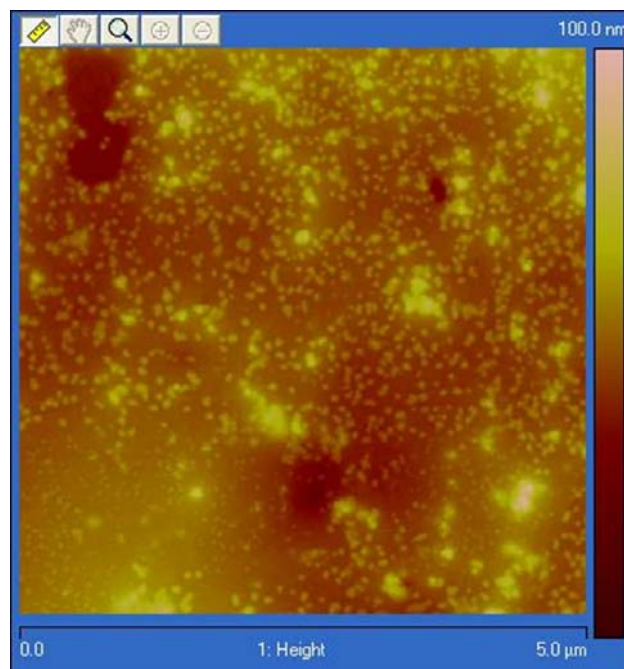


**Fig. 15:** AFM of spherical AuNPs.

#### **Catalase (CAT) (U/mL)**

CAT is antioxidant enzyme that is present in most aerobic cells. It serves as one of the body's defence systems against  $H_2O_2$ , which is a strong oxidant that can cause intracellular damage.

2- As shown in table 3 and fig. 8, the CAT activity in the plasma of diabetic rats was significantly decreased compared with the controls (0.14 vs. 0.21 U/mL;  $P < 0.001$ ). After the use of AuNPs in the diabetic rats, a significant increase in the plasma CAT activity was observed compared with the control rats (0.50 vs. 0.21 U/mL;  $P < 0.000$ ). However, there was a significant increase in the CAT activity after AuNP treatment of the STZ-induced diabetic rats compared with the DC rats

(0.50 vs. 0.14U/mL;  $P < 0.001$ ). Table 3 clearly demonstrates that this parameter yielded a decreased level (64.68% as a percentage of the control level); however, the CAT activity in all of the samples examined in the DT and NT groups was increased (fig. 7), which was demonstrated by the percentage change compared with the control (199.25% and 235.23%, respectively), thereby reflecting the effects of the AuNPs and their antioxidative benefits in the DT group.

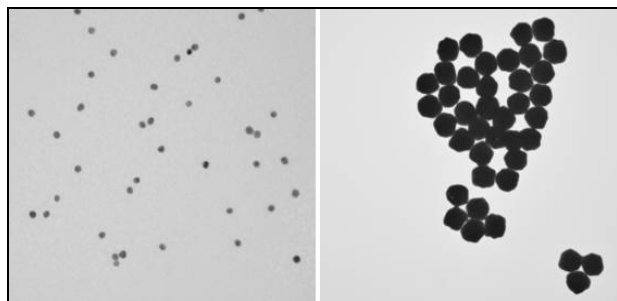


**Fig. 16:** TEM images of 5nm (left) and 400nm (right) AuNPs with <4% CV.

#### **Glutathione peroxidase (GPx) (U/L)**

Cellular GPx is a member of the family of GPx enzymes whose function is to detoxify peroxides in the cell. Because peroxides can decompose to form highly reactive free radicals, the GPx enzymes play a critical role in protecting the cell from free radical damage, particularly lipid per oxidation.

3- table 3 and fig. 6 show an obvious, significant elevation in the GPx activity in DT rats and NT compared with the control rats (70.58 and 83.77, respectively, vs. 39.82 U/L;  $P < 0.001$ ). The results indicate that DC rats exhibit a lower enzymatic activity level compared with the control value (19.16 vs. 39.82 U/L). The table reveals that this parameter exhibited significantly increased levels in the DC rats compared with the DT rats (19.16 vs. 70.58 U/L;  $P < 0.001$ ). Moreover, there was a highly significant difference between the means of the compared groups. The percentage change between the control (fig. 7) and the Group II rats revealed a decreased level of GPx (48.12% as a percentage of the control level), but this marker exhibited an increased level in the Groups III and IV rats (177.27% and 210.38% as a percentage of the control level, respectively), which supports the protective effect of AuNPs on lipid per oxidation.

#### **Glutathione reductase (GR) (U/L)**

GR catalyses the reduction of GSSG to GSH. GR is essential for the glutathione redox cycle that maintains adequate levels of cellular GSH, which acts as an antioxidant.

4- The significant reduction in the plasma GR activity in diabetic rats compared with the control rats is shown in

table 3 and fig. 8 (0.70 vs. 2.00 U/L;  $P < 0.001$ ). It was evident that the mean GR values in the DT group and NT group were higher than in the DC rats. However, there was no significant difference between the NT rats and control rats (1.58 vs. 2.00 U/L;  $P > 0.05$ ). After the use of AuNPs in the STZ-induced diabetic rats, a significant increase in the plasma GR activity was observed compared with the DC rats (1.87 vs. 0.70 U/L;  $P < 0.001$ ). The AuNP treatment was effective, as demonstrated by the increased GR levels exhibited between the control group (fig. 7) and Groups III and IV rats (78.64% and 93.41% as a percentage of the control level, respectively) even as the STZ-induced diabetic rats demonstrated decreased GR levels.

#### **Oral glucose tolerance test (OGTT)**

For the OGTT, 1g/kg bw of glucose dissolved in water was fed to the overnight-fasted mice, and the blood glucose level was determined after 120 min. The fasting blood glucose (FBG) levels after the oral administration of glucose in the control and experimental animals are presented in fig. 9. The FBG levels estimated in the diabetic mice were significantly elevated. However, this level was reduced significantly upon treatment with AuNPs at a dosage of 2.5mg/kg bw/day (fig. 9). The blood glucose level had decreased significantly by 90 min compared with an elevated level at 30min and this decreased level was maintained until 120min with an effective dose of AuNPs ( $P < 0.05$ ).

## **DISCUSSION**

The present study is the first to demonstrate that AuNPs significantly enhance antioxidant production in STZ-induced diabetic rats, which is a recognised model of type 1 diabetic mellitus (T1DM). In addition to changes in blood glucose levels, oxidative stress induced by hyperglycaemia leads to the activation of stress-signalling pathways, which worsen both insulin secretion and action and promote the development of type 2 diabetic mellitus (T2DM) (Evans *et al.*, 2002). The present study indicates a significant improvement in diabetes biomarkers, including markers of oxidative stress, kidney function and liver function. A relative improvement in these biomarkers was demonstrated following treatment with AuNPs in STZ-induced diabetes rats or when used separately. Hyperglycaemia caused by diabetes is known to be a cause of oxidative stress that leads mainly to the enhanced production of mitochondrial ROS (Brownlee, 2001, Jay *et al.*, 2006 and Kowluru, Chan 2007). Similarly, oxidative stress and damage to the tissues and blood in STZ-induced diabetic rats enhance glucose auto oxidation and may contribute to the complications associated with diabetes (Kowluru and Chan 2007). A recent study reported that lipid per oxidation levels were elevated and that the activity levels of antioxidant enzymes (SOD, GPx and CAT) were significantly reduced in STZ-induced diabetic rats (Jin *et al.*, 2008).

**Table 5:** Comparison between the control, DC, DT and NT groups with respect to the glucose (mg/dL), BUN (mg/dL), creatinine (mg/dL) and uric acid (mg/dL) levels.

Parameters	Groups	N	Mean $\pm$ SD	P value <sup>a</sup>	P value <sup>b</sup>	P value <sup>c</sup>	Percent change compared with control
Glucose (mg/dL)	Control	5	97.60 $\pm$ 17.30	-----	-----	<0.001	100.00
	DC	5	450.80 $\pm$ 65.65	<0.001	<0.001		461.89
	DT	5	214.60 $\pm$ 21.24	<0.001			119.87
	NT	5	96.20 $\pm$ 11.28	>0.05	-----		98.57
BUN (mg/dL)	Control	5	26.60 $\pm$ 5.73	-----	-----	<0.001	100.00
	DC	5	47.60 $\pm$ 5.18	<0.001	<0.001		185.94
	DT	5	25.20 $\pm$ 3.03	>0.05			94.73
	NT	5	18.80 $\pm$ 2.77	<0.05	-----		73.44
Creatinine (mg/dL)	Control	5	0.31 $\pm$ 0.03	-----	-----	<0.001	100.00
	DC	5	0.62 $\pm$ 0.05	<0.001	<0.001		200.00
	DT	5	0.33 $\pm$ 0.04	>0.05			105.13
	NT	5	0.27 $\pm$ 0.07	>0.05	-----		85.90
Uric Acid (mg/dL)	Control	5	2.24 $\pm$ 0.54	-----	-----	<0.001	100.00
	DC	5	3.44 $\pm$ 0.30	<0.001	<0.001		153.57
	DT	5	2.20 $\pm$ 0.12	>0.05			98.21
	NT	5	1.94 $\pm$ 0.21	>0.05	-----		86.61

<sup>a</sup>P value between the control group and the DC, DT and NT groups, <sup>b</sup>P value between the DC group and the DT group, <sup>c</sup>P value between all groups

Table 5 describes the following: The independent t-test between the control group and the DC, DT and NT groups with respect to the glucose (mg/dL), BUN (mg/dL), creatinine (mg/dL) and uric acid (mg/dl) levels.

The independent t-test between the DC group and the DT group with respect to the glucose (mg/dL), BUN (mg/dL), creatinine (mg/dL) and uric acid (mg/dL) levels.

Percentage change compared with control for the DC, DT and NT groups with respect to the glucose (mg/dL), BUN (mg/dL), creatinine (mg/dL) and uric acid (mg/dL).

Therefore, we further examined the antioxidative effects of AuNPs in STZ-induced diabetic rats and found that the lipid per oxidation levels, liver function, and kidney function in the diabetic rats were significantly improved by AuNP treatment. We have shown for the first time in STZ-induced type 1 diabetic rats that there is a decrease in the blood glucose levels after the initiation of AuNP treatment. We also demonstrated a significant reduction in the peak blood glucose levels within two hours during an OGTT, which confirms the anti-diabetogenic potential of AuNPs in the rat model. Furthermore, the AuNPs at a dosage of 2.5 mg/kg bw significantly decreased the blood glucose level and improved kidney function results on blood parameter analyses to ranges comparable to the DC groups, in accordance with previous research. The levels of creatinine, BUN and uric acid, which indicate normal renal function, were also restored to near normal levels in the DT rats, suggesting a role for AuNPs in preventing kidney damage. These restorative and non-toxic effects of AuNPs on the serum clinical chemistry correlate with previous experimental evidence using AuNPs to enhance radiotherapy results in mice treated with AuNPs for 11 and 28 days; the animals did not exhibit any significant changes compared with the control mice (Hainfeld *et al.*, 2004). Furthermore, in the present study, we demonstrated that diabetic rats receiving AuNP treatment had significantly increased SOD, GPX, GR and CAT

levels compared with the DC group. The only side effects of the AuNPs observed in this study namely, partial elevation of the mean glucose levels in the blood might occur because of enhanced STZ cytotoxicity due to AuNP administration. However, AuNP treatment in the Group IV rats significantly lowered their mean glucose level, and no significant difference was observed compared with the control group, suggesting that the AuNPs restrained the blood glucose level to near the level in the controls. In fact, a clear link between oxidative stress and diabetes exists, and the liver is the main organ involved because the liver is rich in mitochondria that perform metabolic functions. Oxidative stress has been identified as a likely mechanism of nanoparticle toxicity (Li *et al.*, 2008). Because the liver is an important organ for iron storage, it may be more susceptible to lipid per oxidation than other tissues. AuNPs are taken up by the Kupffer cells of the liver, and their bioaccumulation is regulated by the reticuloendothelial system (Siddiqi *et al.*, 2012). The liver plays an important role in glucose metabolism, and in a chronic hyperglycaemic state, liver oxidative stress is considered a relevant process. Oxidative stress induced by hyperglycaemia leads to liver cell damage because the liver is subject to ROS-mediated injury in diabetes. In the present study, a significant reduction in plasma antioxidant enzymes was observed, and this finding is supported by previous reports, as mentioned above. In

contrast, ROS play an important role in the regulation of hepatic glucose production. The effect of AuNPs in our investigation combined with the effect of the anti-diabetic drugs that act through the inhibition of hepatic gluconeogenesis produce concurrent antioxidant effects that are beneficial in the treatment of diabetes (Hoseini and Esmaily 2006). In diabetes, increased ROS coupled with depolarisation of the inner mitochondrial membrane reduces the availability of ATP. Considering the large number of mitochondria present in the liver, a reduction in hepatic ATP production under diabetic conditions appears to be the result of abnormal lipid metabolism and hyperglycaemia, which may promote lipid per oxidation (Li *et al.*, 2008). Oxidative stress in diabetes mellitus has been linked to improved production of super oxide anion by mitochondria (Nishikawa *et al.*, 2000) and protein kinase C-dependent activation of membranous nicotinamide adenine dinucleotide phosphate (NADPH) oxidase (Inoguchi *et al.*, 2000). The activation of these pathways is linked not only to the development of the late complications of diabetes but also to insulin resistance and  $\beta$ -cell dysfunction (Evans *et al.* 2002). Diabetes has also been implicated in the activation of several stress-activated signalling pathways that include nuclear factor-kappaB (NF- $\kappa$ B), NH<sub>2</sub>-terminal Jun kinases/stress activated protein kinases (JNK/SAPK), p38 mitogen-activated protein (MAP) kinase and hexosamine. The potential antioxidant properties of AuNPs in controlling oxidative stress-mediated lipid per oxidation, which were observed in the present study, might be due to the inhibitory activity of AuNPs in one of the above-mentioned pathways because nanoparticles are known to selectively enter cells damaged due to oxidative stress and to potentially inhibit apoptosis by hindering the JNK pathway (Lao *et al.*, 2009). Moreover, the interaction of the AuNPs with the cysteine residues of thioredoxin (a highly conserved thiol reductase that acts on an endogenous inhibitor, thioredoxin-interacting protein (Txnip)), thereby preventing the inhibitor protein Txnip from binding to it under high glucose levels. The binding reaction between the gold's surface and the cysteine residues in the protein is highly stable (Junn *et al.*, 2000). The regulation of the cellular redox balance is responsible for the antioxidative mechanism. Thioredoxin reflects the other concept that the antioxidant properties of AuNPs involve their interaction with thioredoxin. A cysteine thiol group is also the active site of certain enzymes. Abnormally elevated thiols may possibly affect protein synthesis or enzyme function through disulphide bonding to the cysteinyl groups at structurally or enzymatically important sites or by acting on existing disulphide bridges. The role of the thiol redox couple in maintaining the normal structure and function of many enzymatic and non-enzymatic antioxidants affects the blood sugar levels. Elevated cysteine levels can interact with immunoglobulins and components of the complement pathway to reduce the clearance of immune complexes, a

process that may be important in autoimmune-related diseases such as T1DM (Bradley *et al.*, 1994). Our results are in agreement with the study of Siddiqi *et al.* (2012). The authors demonstrated a significant increase in reduced glutathione and catalase, which may have been due to increased lipid peroxidation after AuNP treatment. According to another author (Hung *et al.*, 2004). The non-significant change in the mean activity of GR in the Group IV rats compared with the control rats (table 3 and fig. 8) in our results might be explained by the fact that GR activity is sufficient to maintain an elevated reduced/oxidised GSH ratio under physiological conditions. However, excessive intracellular oxidative stress exceeding the capacity of GR will induce the export of GSSG (oxidised glutathione) to the plasma in an attempt to regain intracellular redox homeostasis. During the detoxification process, GSH (reduced form) becomes oxidised glutathione (GSSG), which is then recycled to GSH by the enzyme GR present in cells. Decreased destruction by antioxidants such as GR, SOD, CAT and GPx may result in increased ROS levels [29]. In conclusion, AuNPs show beneficial antioxidative effects in experimentally induced diabetes. Therefore, this combination should be analysed in further tests and clinical trials.

## CONCLUSIONS

The findings of this study suggest that treatment with 2.5 mg/kg bw/day of AuNPs does not cause any oxidative stress in T1DM. Further studies are warranted to examine the effects of a broader dose range of AuNPs on the time course of free radical indices in T1DM with different disease in rats to establish a clearer understanding of the bio safety of AuNPs.

## ACKNOWLEDGEMENTS

This research project was supported by a grant from the "Research Center of the Female Scientific and Medical Colleges," Deanship of Scientific Research, King Saud University.

## REFERENCES

- Aebi H (1984). Catalase *in vitro*. *Methods Enzymol.*, **105**: 121-126.
- Aronson D (2008). Hyperglycemia and pathobiology of diabetic complications. *Adv. Cardiol.*, **45**: 1-16.
- Bradley H, Gough A, Sokhi RS, Hassell A, Waring R and Emery P (1994). Sulfate metabolism is abnormal in patients with rheumatoid arthritis. Confirmation by *in vivo* biochemical findings. *J. Rheumatol.*, **21**: 1192-1196.
- Brownlee M (2001). Biochemistry and molecular cell biology of diabetic complications. *Nature*, **414**: 813-820.

- Calam RR (1988). Specimen processing separator gels: An update. *J. Clin. Immunoassay*, **11**: 86-90.
- Chang TI, Horal M, Jain S, Wang F, Patel R, Loeken MR (2003). Oxidant regulation of gene expression and neural tube development: Insights gained from diabetic pregnancy on molecular causes of neural tube defects. *Diabetologia*, **46**: 538-545.
- Evans JL, Goldfine ID, Maddux BA and Grodsky GM (2002). Oxidative stress and stress-activated signaling pathways: A unifying hypothesis of type 2 diabetes. *Endocr. Rev.*, **23**: 599-622.
- Fossati P, Prencipe L and Berti G (1980). Use of 3,5-dichloro-2-hydroxybenzenesulfonic acid/4-aminophenazone chromogenic system in direct enzymic assay of uric acid in serum and urine. *Clin. Chem.*, **26**: 227-231.
- Goldberg DM and Spooner RJ (1983). Assay of glutathione reductase. In *Methods of Enzymatic Analysis*. 3<sup>rd</sup> edition. Edited by Bergmeyer HU, Bergmeyer J, Grassl M. Deerfield Beach, FL: Verlag Chemie. Pp.258-265.
- Guo R, Song Y, Wang G and Murray RW (2005). Does core size matter in the kinetics of ligand exchanges of monolayer-protected Au clusters? *J. Am. Chem. Soc.*, **127**: 2752-2757.
- Hainfeld JF, Slatkin DN and Smilowitz HM (2004). The use of gold nanoparticles to enhance radiotherapy in mice. *Phys. Med. Biol.*, **49**: 309-315.
- Harrison D, Griendling KK, Landmesser U, Hornig B, Drexler H (2003). Role of oxidative stress in atherosclerosis. *Am. J. Cardiol.*, **91**(3A): 7A-11A.
- Hoseini S, Esmaily H, Mohammadirad A, Abdollahi M (2006). Effects of sildenafil a phosphodiesterase 5 inhibitor on rat liver cell key enzymes of gluconeogenesis and glycogenolysis. *Int. J. Pharmacol.*, **2**: 280-285.
- Hung RG, Boffetta P, Brennan C, Malaveille A, Donato F (2004). GST, NAT, SULT1A1, CYP1B1 genetic polymorphisms, interactions with environmental exposures and bladder cancer risk in a high-risk population. *Int. J. Cancer*, **110**: 4598-4604.
- Inoguchi T, Li P, Umeda F, Yu HY, Kakimoto M, Imamura, M, Aoki T, Etoh T, Hashimoto T, Naruse M, Sano H, Utsumi H and Nawata H (2000). High glucose level and free fatty acid stimulate reactive oxygen species production through protein kinase c-dependent activation of nad(p)h oxidase in cultured vascular cells. *Diabetes*, **49**: 1939-1945.
- Jay D, Hitomi H and Griendling KK (2006). Oxidative stress and diabetic cardiovascular complications. *Free Radic. Biol. Med.*, **15**: 183-192.
- Jeon KI, Byun MS and Jue DM (2003). Gold compound auranofin inhibits Ikappa B kinase (IKK) by modifying Cys-179 of IKKbeta subunit. *Exp. Mol. Med.*, **35**: 61-66.
- Jin L, Xue HY, Jin LJ, Li SY and Xu YP (2008). Antioxidant and pancreas-protective effect of aucubin on rats with streptozotocin-induced diabetes. *Eur. J. Pharmacol.*, **582**: 162-167.
- Junn E, Han SH, Im JY, Yang Y, Cho EW, Um HD, Kim DK, Lee KW, Han PL, Rhee SG and Choi I (2000). Vitamin D3 up-regulated protein 1 mediates oxidative stress via suppressing the thioredoxin function. *J. Immunol.*, **164**: 6287-6295.
- Kalishwaralal K, Deepak V, Pandian SRK and Gurunathan S (2009). Biological synthesis of gold nanocubes using *Bacillus licheniformis*. *Bioresour. Technol.*, **100**: 5356-5358.
- Kneipp J, Kneipp H, Rice WL and Kneipp K (2005). Optical probes for biological applications based on surface-enhanced Raman scattering from indocyanine green on gold nanoparticles. *Anal. Chem.*, **77**: 2381-2385.
- Kowluru RA and Chan PS (2007). Oxidative stress and diabetic retinopathy. *Exp. Diabetes Res.*, p.43603.
- Lao F, Chen L, Li W, Ge C, Qu Y, Sun Q, Zhao Y, Han D and Chen C (2009). Fullerene nanoparticles selectively enter oxidation-damaged cerebral micro vessel endothelial cells and inhibit JNK-related apoptosis. *ACS Nano.*, **3**: 3358-3368.
- Lee MY, Park SJ, Choi JS, Oh MK and Kim IS (2007). Auranofin blocks interleukin-6 signalling by inhibiting phosphorylation of JAK1 and STAT3. *Immunology*, **122**: 607-614.
- Li N, Xia T and Nel AE (2008). The role of oxidative stress in ambient particulate matter-induced lung diseases and its implications in the toxicity of engineered nanoparticles. *Free Radic. Biol. Med.*, **44**: 1689-1699.
- Mukherjee P, Bhattacharya R, Wang P, Wang L, Basu S, Nagy JA, Atala A, Mukhopadhyay D and Soker S (2005). Antiangiogenic properties of gold nanoparticles. *Clin. Cancer Res.*, **11**: 3530-3534.
- Nishikawa T, Edelstein D, Du XL, Yamagishi SI, Matsumura T, Kaneda Y, Yorek MA, Beebe D, Oates PJ, Hammes HP, Giardino I and Brownlee M (2000). Normalizing mitochondrial super oxide production blocks three pathways of hyperglycaemic damage. *Nature*, **404**: 787-790.
- Nishikimi M, Roa NA and Yogi K (1972). Measurement of superoxide dismutase. *Biochem. Biophys. Res. Commun.*, **46**: 849-854.
- Norton S (2008). A brief history of potable gold. *Mol. Interv.*, **8**(3): 120-125.
- Paglia DE, Valentine WN (1967). Studies on the quantitative and qualitative characterization of erythrocyte glutathione peroxidase. *J. Lab. Clin. Med.* **70**: 158-169.
- Reasner CA (2008). Reducing cardiovascular complications of type 2 diabetes by targeting multiple risk factors. *J. Cardiovasc. Pharmacol.*, **52**: 136-144.

- Scheen JA (1997). Drug treatment of non-insulin dependent diabetes mellitus in the 1990s. Achievements and future development. *Drugs*, **54**: 355-368.
- Siddiqi NJ, Kasim MA, AlYafee YA, Alhomida AS (2012). Studies on the effect of gold nanoparticles on oxidative stress and antioxidants defense indices in various rat tissues. *Afr. J. Pharm. Pharmacol.*, **6**(47): 3246-3251.
- Tietz NW (1987). *Fundamentals of Clinical Chemistry*. 3<sup>rd</sup> edition. Philadelphia WB Saunders, pp.369-371.
- Vinik AI and Vinik E (2003). Prevention of the complications of diabetes. *Am. J. Manage Care*, **9**: S63-S80.
- Wild S, Roglic G, Green A, Sicree R and King H (2004). Global prevalence of diabetes. *Diabetes Care*, **27**: 1047-1053.
- Wolffe SP, Jiang ZY and Hunt JV (1991). Protein glycation and oxidative stress in diabetes mellitus and ageing. *Free Radic. Biol. Med.*, **10**: 339-352.